

Systemic therapy with the infectivity-selective oncolytic adenovirus by targeting mesothelin

Mizuho Sato-Dahlman,^{1,2} Yoshiaki Miura,¹ Praveensingh Hajeri,¹ Brett Roach,¹ Kari Jacobsen,¹ and Masato Yamamoto^{1,2}

¹Department of Surgery, University of Minnesota, Minneapolis, MN, USA; ²Masonic Cancer Center, University of Minnesota, Minneapolis, MN, USA

Treatment of advanced stage cancers is extremely challenging, and more effective systemic therapy is needed. Oncolytic adenoviruses (OAd) are one of the most promising anti-cancer agents. However, systemic delivery of OAd is challenging due to the low transduction in tumor cells caused by non-selective distribution and sequestration by non-target organs. To overcome this issue, we have previously generated a mesothelin (MSLN)-targeted OAd (AdML-VTIN). Here, we are reporting the potential of MSLN-targeted OAd as an agent for novel systemic treatment using MSLN-expressing lung and pancreatic cancer models. The *in vivo* biodistribution of AdML-VTIN after intravenous injection showed significantly lower liver sequestration compared to the wild type of OAd (AdML-5WT). By day 7, the intratumoral viral copy number of AdML-VTIN was significantly higher than that of AdML-5WT. For therapeutic efficacy, systemically injected AdML-VTIN exhibited statistically significant anti-tumor effects in both lung and pancreatic cancer xenograft tumor models. In addition, we tested the effect of preexisting immunity using human serum. In a neutralization assay, AdML-VTIN was more resistant to preexisting antibodies, compared to Ad5-WT. Interestingly, the hemagglutination profile of AdML-VTIN was also changed. Our results indicate that MSLN-targeted OAd has great potential to facilitate systemic therapy of advanced cancers.

INTRODUCTION

Despite recent advances in cancer diagnostic technologies, many cancer patients are still initially diagnosed with advanced disease.^{1,2} Among them, lung cancer is the most common cause of death from cancer, and most deaths are associated with metastatic disease. Unfortunately, more than 50% of newly diagnosed lung cancer patients have metastatic disease.³ The 5-year survival rate for metastatic lung cancers is 7%.⁴ Pancreatic cancer is also an aggressive malignant disease and is predicted to become the 2nd leading cause of cancer death before 2030.⁵ Surgical resection combined with chemotherapy remains the mainstay of curative treatment for pancreatic cancer; however, fewer than 20% of patients are candidates for surgery because the cancer has usually spread beyond the pancreas by the

time it is diagnosed.⁶ Therefore, treatment of these late-stage cancers is extremely challenging, and a more effective systemic therapy is needed.

Gene therapy/virotherapy strategies show great promise in providing new options for the treatment of various cancers. One such virus, talimogene laherparepvec (T-VEC, Imlygic, Amgen),⁷ was approved as the first virotherapy in the United States for metastatic melanoma with intratumoral (i.t.) injection. The adenovirus (Ad) is one of the most widely used viral backbones for the development of oncolytic viruses (OVs) due to its high *in vivo* transduction efficiency.^{8–19} Oncolytic adenoviruses (OAd) show an anti-tumoral effect via their i.t. amplification and strong cytotoxic effects in a variety of cancers.^{20–23} However, the systemic delivery of OAd is challenging due to the low transduction in tumor cells caused by non-selective distribution and sequestration by non-target organs, such as liver, and viral inactivation by neutralizing antibodies (nAbs).^{24,25} The realization of systemic oncolytic virotherapy mandates a more efficient and selective delivery of the functional viruses to the tumor for sufficient antitumor effect. The targeting of the OV at the level of infection (transductional targeting) should therefore potentiate the antitumor effect of OAd by improving the initial tumor site localization after systemic administration, as well as tumor-selective viral replication and spread in the tumor.

We previously developed a mesothelin (MSLN)-targeted OAd using an Ad library screening system.²⁶ MSLN is a cell surface glycoprotein that is highly expressed on several malignant tumors (e.g., lung cancer, pancreatic cancer, ovarian cancer, mesothelioma), while little or no expression has been detected in normal tissues.^{26–29} The MSLN-targeted OAd showed not only a selectivity for MSLN-expressing cells *in vitro* but also a selective and potent *in vivo* antitumor effect resulting from viral replication in MSLN⁺ xenografts.²⁶

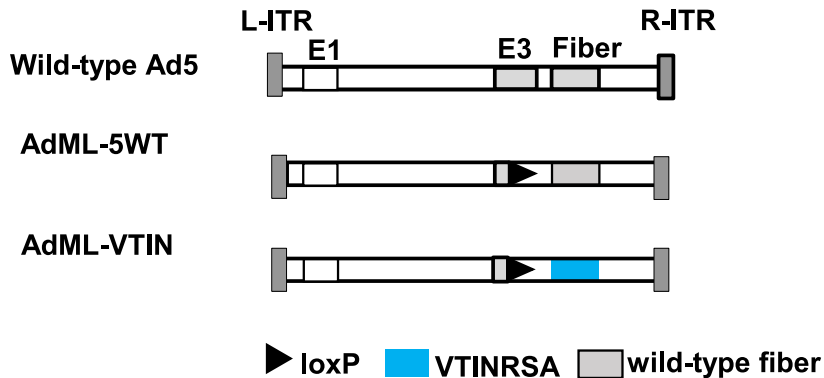
Received 30 January 2025; accepted 12 March 2025;
<https://doi.org/10.1016/j.omton.2025.200967>.

Correspondence: Masato Yamamoto, Division of Basic and Translational Research, Department of Surgery, University of Minnesota, MMC195, 420 Delaware Street SE, Minneapolis, MN 55455, USA.

E-mail: yamam016@umn.edu



A Structure of adenoviruses



B AB-loop of Adenovirus



Here, we evaluated for the first time the possibility of using MSLN-targeted OAds for systemic treatment in lung cancer and pancreatic cancer models. Targeting of MSLN at the level of binding and infection via the Ad fiber modification results in a strong therapeutic effect in both lung cancer and pancreatic cancer subcutaneous xenograft models. The *in vivo* biodistribution of AdML-VTIN after intravenous (i.v.) injection showed significantly lower liver sequestration compared to wild-type (WT) Ad5. Moreover, modification of the Ad fiber reduced neutralization by preexisting nAbs and hemagglutination activity of Ad.

These data suggest that MSLN-targeted OAds are a very promising agent for the development of systemic therapy for advanced refractory cancers.

RESULTS

Distribution of MSLN-targeted OAds

To achieve cancer cell-selective binding and infection for an Ad, we have generated an MSLN-targeted infectivity-selective OAd in previous studies via our binding-based screening system with a high-diversity Ad-formatted fiber library.²⁶ MSLN is a cell surface glycoprotein that is highly expressed in lung cancer, pancreatic cancer, ovarian cancer, and mesothelioma.^{26–30} By using our library screening system, the MSLN-targeted OAd, AdML-VTIN, was isolated.²⁶ AdML-VTIN has a WT E1 gene, a single *loxP* site within the E3 region, and the MSLN-targeting motif (VTINRSA) replacing the primary coxsackievirus and Ad receptor (CAR)-binding domain in the AB-loop of the fiber knob (Figure 1). The resultant virus with *loxP* site is therefore E3

Figure 1. Mesothelin-targeted oncolytic adenovirus

(A) Schematic representation of fiber-remodeled adenoviruses (Ads). AdML series of the viruses has a wild-type (WT) E1 gene, a single *loxP* site replacing the E3 gene, and targeting motif in the AB-loop regions of the fiber. (B) Amino acid sequence of mesothelin (MSLN)-targeted Ad (AdML-VTIN), and non-targeted Ad (AdML-5WT) fibers.

deficient. AdML-VTIN showed selective binding and cytotoxicity for MSLN-expressing pancreatic cancer cells *in vitro* and *in vivo*.²⁶

Because the change in the original receptor binding site was expected to redefine the vector binding profile of AdML-VTIN, the organ distribution of AdML-VTIN and AdML-5WT (Ad with WT Ad5 fiber) was assessed after tail vein injection of nude mice with MSLN⁺ subcutaneous tumor at 1×10^{10} vector particles (vp)/mouse. As a proof-of-concept study, we used the human lung cancer cell line A549 and the human pancreatic cancer cell line AsPC1 in this paper, and both of the cells

generated MSLN⁺ tumors in nude mice (Figure S1). When AdML-VTIN was injected into the tail vein of nude mice carrying A549 subcutaneous xenografts, liver distribution was remarkably lower than that of AdML-5WT at 1 h and 48 h after administration (Figures 2A and 2B). While there was no statistically significant difference between AdML-5WT and AdML-VTIN in the tumor at 1 h (Figure 2A), the viral copy number of AdML-VTIN in the tumor was about 3 times and 10 times higher than that of AdML-5WT at 48 h and 7 days, respectively. (Figure 2B). These data indicated that the OAd with a redesigned AB-loop changed liver tropism and replicated in the tumor.

Viral distribution in primary mouse liver cells

Next, we investigated the cellular distribution of AdML-VTIN in the liver tissue. A total of 3×10^9 vp of AdML-VTIN and AdML-5WT were systemically injected into nude mice. One hour after administration, we examined the vector distribution of AdML-VTIN and AdML-5WT to liver parenchymal cells or non-parenchymal cells, which were isolated by differential centrifugation using Percoll after collagenase digestion.³¹ In flow cytometry, Kupffer cells, which are positive in F4/80, were seen in the non-parenchymal cell fraction, but not in the parenchymal cell fraction (Figure 3A). Then, we measured the viral copy number in each fraction by quantitative PCR (qPCR). The vector distribution of AdML-VTIN to the parenchymal cell fraction was significantly lower than that of AdML-5WT, while the vector distribution of AdML-VTIN to the non-parenchymal cell was at a level similar to that of AdML-5WT (Figure 3B). These results suggest that the redesigned fiber enabled escape from sequestration by liver parenchymal cells.

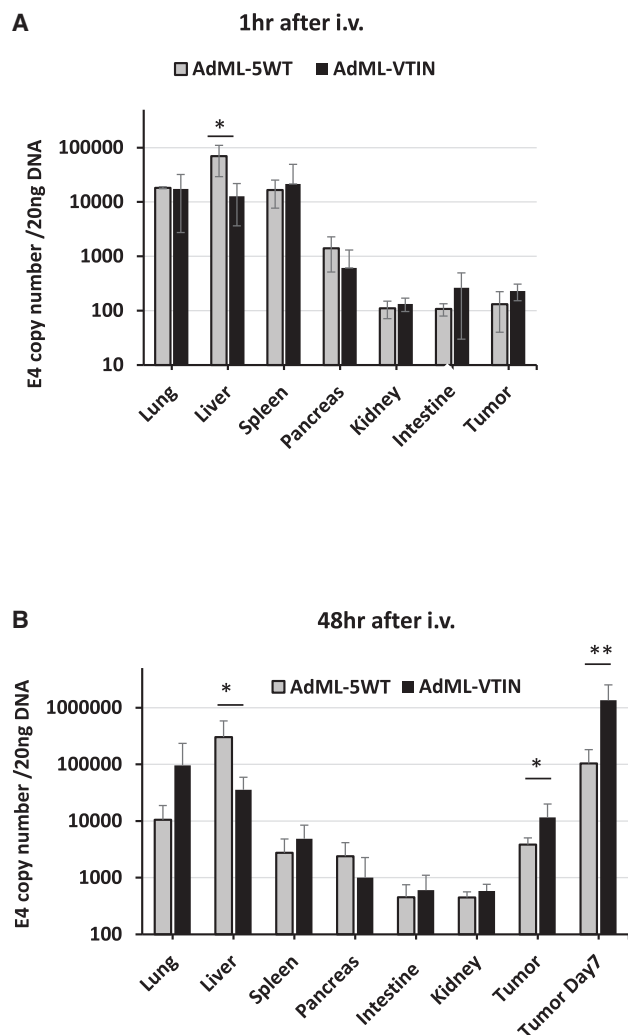


Figure 2. *In vivo* distribution of the MSLN-targeted Ad

To analyze the vector distribution, 2×10^7 of A549 cells were inoculated subcutaneously into the flank of female nude mice, and 3×10^9 vp of the targeted or control virus was systemically injected when the tumor diameters reached 5–7 mm. (A) One hour after injection; $n = 3$. (B) Forty-eight hours after injection; $n = 4$. The data were analyzed using a two-tailed unpaired Student's *t* test. * $p < 0.05$; ** $p < 0.01$.

Anti-tumor effect of systemic administration and i.t. direct injection of AdML-VTIN

Next, we compared the anti-tumor effect of AdML-VTIN between i.v. and i.t. injections using a subcutaneous xenograft model with an MSLN⁺ tumor (A549). When tumors reached 5–7 mm in diameter, 3×10^9 vp AdML-VTIN was injected via i.v. or i.t. AdML-VTIN injection resulted in significant initial tumor volume reduction as well as longer-term suppression of the tumor growth in both i.v. and i.t. administrations (Figure 4A). Importantly, no difference was observed between the antitumor effects of i.v. and i.t. administrations.

To investigate the replication and i.t. spread of the virus, we performed a separate experiment in A549 tumors with the same setup. Tumor samples at days 5 and 8 were assessed for viral copy number and viral structural protein (hexon) staining. Five days after i.t. treatment with AdML-VTIN, a high level of hexon expression was restricted to a certain area of the tumor, which is assumed as a needle track. In the tumor with i.v. injection, although scattered cells showed strong signal of hexon, we observed weak signal of hexon expression in a broader area of the tumor (Figure 4B, left). At day 8, both systemic injection and i.t. injection resulted in high levels of hexon expression. The presence of hexon-positive cells became equivalent between i.v.- and i.t.-injected groups, and the distribution after i.v. injection appeared more homogeneous in the tumor (Figure 4B, right).

We also subsequently assessed the virus DNA copy number by E4 qPCR. Although the amount of virus in the tumor with systemic injection was lower than that with i.t. injection at earlier time points (days 1 and 5), the virus copy number in the i.v.-administered group reached the same level of that in the i.t. group at day 8 (Figure 4C).

These results suggest that systemic injection of the MSLN-targeted OAd is equivalently effective compared to an i.t. injection.

Anti-tumor effect of AdML-VTIN versus non-targeted AdML-5WT with systemic injection in MSLN⁺ tumor model

We compared the antitumor effect of MSLN-targeted OAd (AdML-VTIN) and non-targeted OAd (AdML-5WT) in an A549 subcutaneous xenograft model. AdML-VTIN and AdML-5WT were systemically injected into A549 tumor-bearing nude mice. AdML-VTIN via i.v. injection showed tumor shrinkage starting from day 5 and showed the lowest tumor volume for days 8–19. The tumor volume of the AdML-VTIN-treated group was significantly lower than that of AdML-5WT at day 26 (Figure 5A).

Next, we compared viral replication and i.t. viral spread after systemic administration. We performed the same experiment separately to avoid affecting the tumor volume analysis. Expression of viral structural protein (hexon) in tumors was analyzed at day 5. The staining for hexon in the tumor revealed a significant viral distribution in tumors treated with AdML-VTIN at 5 days after administration, while that of AdML-5WT was barely detectable (Figure 5B). The virus copy number in treated tumors was analyzed by qPCR on days 2 and 5 after systemic injection of the viruses. The viral copy number of AdML-VTIN at day 5 was noticeably higher than that of AdML-5WT (Figure 5C). These data indicated that viral replication of MSLN-retargeted OAd was higher compared to non-targeted AdML-5WT in correspondence with the systemic anti-tumor effect. These experiments also confirmed the selectivity and potency of the MSLN-targeted OAd via systemic administration.

Multiple administrations of MSLN-targeted OAd suppressed regrowth of tumors

Interestingly, the plot of individual tumors treated with AdML-VTIN showed that 4 out of 10 tumors showed complete disappearance,

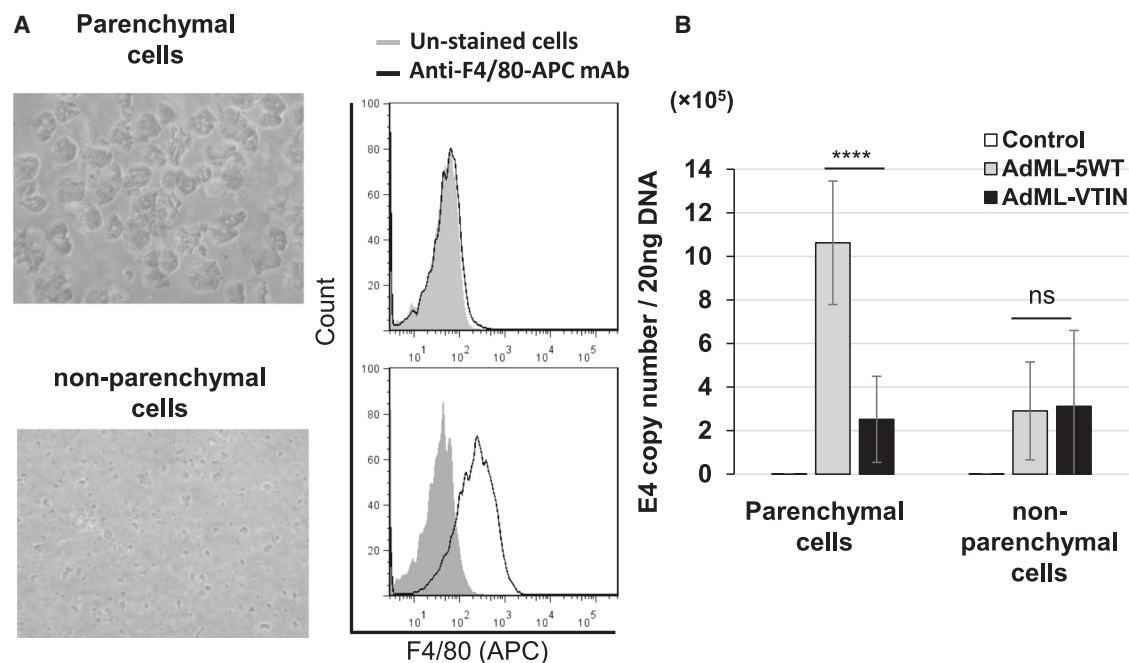


Figure 3. Viral distribution in liver cells

(A) Image of isolated cells: parenchymal cell fraction (top) and non-parenchymal cell fraction (bottom). Flow cytometry analysis with anti-F4/80 showed signals in the non-parenchymal population (Kupffer cells). (B) Viral copy number in each fraction was analyzed by qPCR. The results are shown as E4 copy number per 20 ng DNA. The data were analyzed using a two-tailed unpaired Student's *t* test. *****p* < 0.0001; *n* = 3.

while the remaining tumors showed temporary growth suppression, indicating regrowth of the tumors (Figure S2A). All tumors treated with AdML-VTIN were continuously observed. At day 47, when the average of all tumors reached a volume of 500 mm³, repeated injections of AdML-VTIN against regrown tumors were started. AdML-VTIN via i.v. injection (3×10^9 vp/mouse) was performed on days 47, 61, 68, 75, and 82. The growth of four out of six tumors was significantly suppressed (controlled with repeated AdML-VTIN injection [Figure S2B]). A successful anti-tumor effect at a low dose indicated that an OAd with a targeting motif in the AB-loop had the ability to facilitate systemic therapy.

Anti-tumor effect of systemically injected AdML-VTIN in a pancreatic cancer model

To investigate the treatment effects in pancreatic cancer, we assessed the anti-tumor effect of AdML-VTIN in the human pancreatic cancer cell line AsPC1. The analyses of the MSLN expression levels and CAR by flow cytometry and immunohistochemistry (IHC) revealed that AsPC1 expressed both MSLN and CAR (Figures 6A, S1, and S4). As expected from this, both AdML-5WT and AdML-VTIN showed cytotoxic effects *in vitro*, and the effect of AdML-5WT was slightly stronger from crystal violet staining of the attached cells (Figure 6A). For *in vivo* comparison of the anti-tumor effect of the OAds, AdML-VTIN and AdML-5WT were systemically injected into AsPC1 xenografts when tumors reached 3–5 mm in diameter. In contrast to the *in vitro* analysis, i.v. injection of AdML-VTIN showed a strong inhibition of tumor growth compared to AdML-5WT (Figure 6B).

Next, we compared the viral replication after systemic administration in a pancreatic cancer model. We performed a separate experiment in AsPC1 tumors with the same setup, and the tumor samples were assessed for viral copy number in the tumor by qPCR of the E4 region at 5 and 10 days after systemic injection. Virus replication of AdML-VTIN at both day 5 and day 10 were more than 23 and 12 times higher than that of AdML-5WT, respectively (Figure 6C). These data indicated that MSLN-retargeted OAd showed enhanced therapeutic effect compared to non-targeted OAd in systemic therapy in a pancreatic cancer xenograft model.

The therapeutic effect of AdML-VTIN in the pancreatic cancer PDX mouse model

We assessed the effect of AdML-VTIN in a more clinically relevant model of pancreatic cancer by using patient-derived xenografts (PDXs). To establish the human pancreatic cancer PDX mouse model, surgical samples of human pancreatic cancer were implanted subcutaneously into SCID mice. Once PDX tumors were established, we evaluated the MSLN and CAR expression according to IHC staining intensity. Unlike the A549 tumor, both PDX tumors have high levels of MSLN expression, but the expression level of the Ad receptor, CAR, was low (Figures 7A and S3). Experiments were performed with the PDXs derived from two different patients. When the tumors reached 5–7 mm in diameter, AdML-VTIN and AdML-5WT were systemically injected into PDX-bearing animals. After i.v. administration, only the AdML-VTIN showed significant antitumor effect compared to the untreated group, and the tumor volume after i.v.

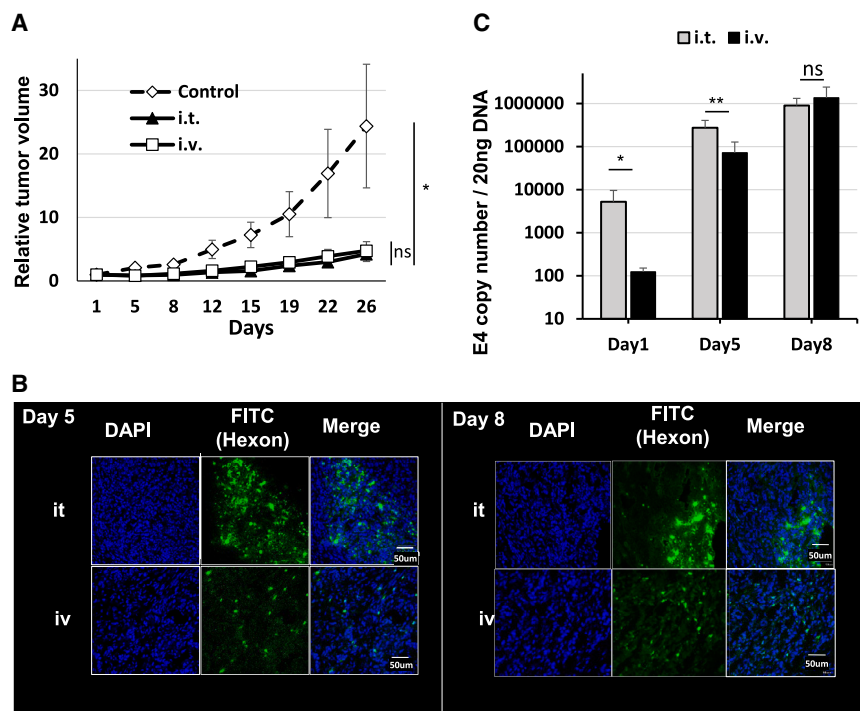


Figure 4. Anti-tumor effect of MSLN-targeted OAd by systemic versus intratumoral injection

(A) The anti-tumor effect of intratumorally or systemically administered MSLN-targeted OAds was analyzed in an A549 subcutaneous xenograft model; 3×10^9 vp/tumor of MSLN-targeted virus (AdML-VTIN) was administered. Mean relative tumor volume \pm SEM; $n = 10$ per group. Significance was calculated by one-way ANOVA analysis followed by Tukey's multiple comparison test. $*p < 0.05$; $n = 5$ mice for each group. (B) At days 5 and 8, the expression of Ad late gene product (hexon) was assessed by immunostaining with the fluorescein isothiocyanate (FITC)-labeled anti-hexon polyclonal antibody (counterstained with DAPI). Staining and sections were performed in at least two independent experiments. Green, Ad hexon protein; blue, nucleus (original magnification, $\times 40$). (C) Viral copy number in the tumor specimens was analyzed by qPCR on days 1, 5, and 8. Results are shown as the E4 copy number per 20 ng DNA. The data were analyzed using a two-tailed unpaired Student's t test. $*p < 0.05$; $**p < 0.01$; $n = 3$ for each time point.

injection of AdML-VTIN was significantly lower than that with AdML-5WT ($p < 0.05$) (Figure 7B). These data suggest that MSLN-targeted OAd can be applicable for the systemic therapy of human pancreatic cancer.

The fiber modification of Ad affected neutralization and hemagglutination activity

We tested the effect of preexisting immunity against the MSLN-targeted OAd in human serum. In a neutralization assay, cell viabilities were measured to examine the impact of human serum on the *in vitro* cell lysis activities of fiber-modified OAds. We performed neutralization assay using serum samples from non-cancer adults from the United States ($n = 6$). At a 1:4 dilution, 5 out of 6 sera showed more than 50% inhibition of WT Ad5 activity (Figure 8A). However, only 2 sera showed >50% inhibition for AdML-VTIN (Figure 8A). These results indicate that a fiber-modified Ad5 vector can escape the neutralizing immune response in human serum.

In addition, we evaluated the hemagglutination activity of AdML-TYML because it has been reported that a major determinant of hemagglutination is the binding of Ad fiber-knob protein to erythrocyte. Ad5-based Ads with CAR-binding knob showed hemagglutination (Figure 8B). In contrast, our AB-loop fiber modified virus (AdML-VTIN) or the fiber-knob replacement virus with Ad3 (Ad5/3), which binds to CD46/DSG-2,^{32,33} did not cause hemagglutination (Figure 8B). This indicates that tropism alternation based on AB-loop modification is an effective way to avoid hemagglutination.

DISCUSSION

OAds show an anti-tumor effect via their i.t. amplification and strong cytotoxic effect in a variety of cancers.^{20–23} However, systemic application of OAd therapy mandates a different kind of efficiency and selectivity of gene delivery, such as organ, and tissue selectivity at the level of transduction. Additionally, there are several obstacles for efficient systemic delivery, such as liver sequestration, nAbs, and stroma. Indeed, Ad vectors injected i.v. into mice are largely sequestered by the liver, and high-dose treatments can lead to liver toxicity.^{25,34–36} One of the reasons for liver tropism is that hepatocytes express high levels of the primary Ad receptor (CAR),^{34,37} and non-parenchymal liver cells (e.g., Kupffer cells, epithelial cells) also capture viral particles.²⁵ As an inevitable consequence of large sequestration of the Ad by the liver, the amount of the virus reaching the tumor becomes low, leading to limited *in vivo* efficacy of systemic therapy.²³ Tumor-selective replication and lateral spread of progeny vectors in the tumors facilitate a dramatic augmentation of the therapeutic effect of OAds,⁹ which can compensate for loss upon systemic delivery to some extent. For the targeting of cancer cells, WT Ad is not a practical choice because many cancer cells have low expression of the Ad primary receptor (CAR).³⁸ Indeed, our PDX tumors showed low expression of CAR (Figure S3). To overcome this issue, infectivity-enhanced OAds with modified fibers have been developed, such as RGD-OAd or Ad5/3.²¹ Although these infectivity-enhanced OAds confer augmented anti-tumor effects in CAR[−] cancers, including pancreatic cancer,^{8,9,39,40} these OAds are not cancer specific^{39,41} and exhibit binding to a variety of normal organs. Even the most advanced infectivity-enhanced OAds that rely on regulations at

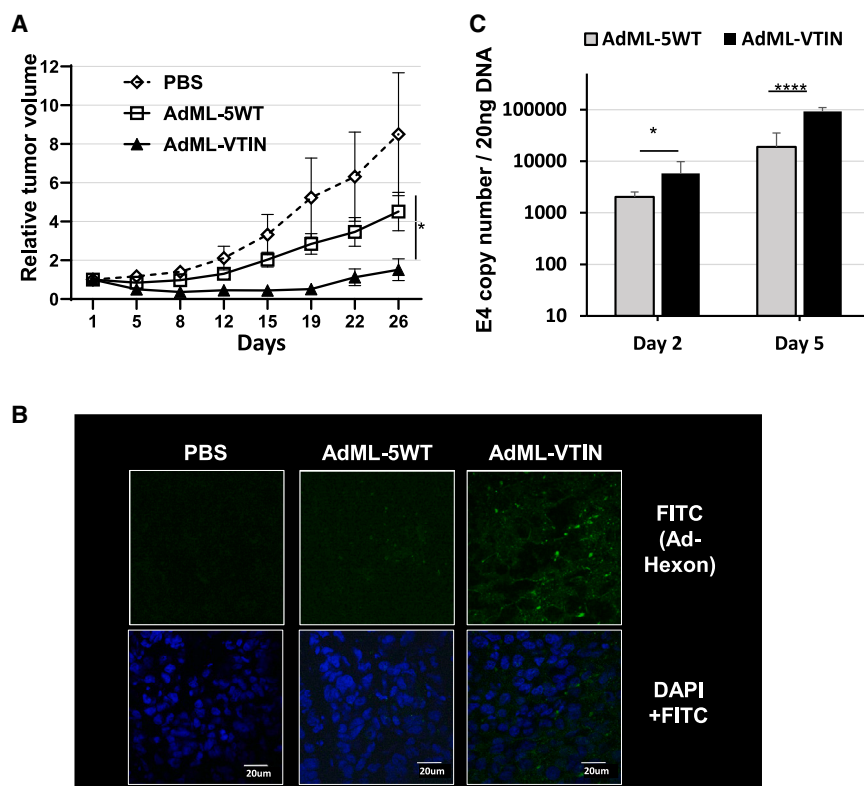


Figure 5. Anti-tumor effect of MSLN-targeted OAd with systemic injection in an MSLN⁺ cancer model

(A) The anti-tumor effect of systemically administered MSLN-targeted and control OAds (3×10^9 vp/mouse) was analyzed in a A549 subcutaneous xenograft model. Results are shown as mean \pm SEM ($n = 10$); two-way ANOVA followed by Tukey's multiple comparisons test. $*p < 0.05$. (B) At day 5, the expression of Ad late gene product (hexon) was assessed by immunostaining with the FITC-labeled anti-hexon polyclonal antibody (counterstained with DAPI). Staining and sections were performed in at least two independent experiments. Green, Ad hexon protein; blue, nucleus (original magnification, $\times 100$). (C) Viral copy number in the tumor specimens was analyzed by qPCR at days 2 and 5. Results are shown as the E4 copy number per 20 ng DNA. The data were analyzed using a two-tailed unpaired Student's *t* test. $*p < 0.05$; $****p < 0.0001$; $n = 4$ for each time point.

the level of replication for cancer selectivity were heavily affected by sequestration in non-target organs (e.g., liver).^{40,42–44}

In this study, we demonstrated that the MSLN-targeted OAd, AdML-VTIN, escapes liver sequestration and achieves better tumor accumulation. While the amount of i.v.-injected virus in MSLN⁺ tumors was initially lower than that of i.t.-injected virus, the viral copy number of the i.v.-injected group caught up with the i.t.-injected group by day 8 (Figure 4C). Because A549 is known to be a cell line that shows the strongest virus replication and therapeutic effect by OAds with WT fiber, the effect of the OAd with VTIN motif replacing the CAR binding domain is quite impressive. These data suggest that a sufficient amount of systemically administered AdML-VTIN accumulated in MSLN⁺ tumors specifically, and also induced an anti-tumor effect via viral replication and spreading within tumors.

A major limitation of systemic administration of Ad type 5 is that the majority of the virus is sequestered by the liver, causing liver damage and systemic toxicity.^{36,45} In terms of liver sequestration, we analyzed biodistribution of the vectors at an early time point (1 h) and at a late time point (48 h), because most of the i.v.-administered Ad is cleared within 24 h.²⁵ Our 1-h data showed that the MSLN-targeted virus, AdML-VTIN, goes to the tumor in the same amount as WT virus, because the tumor (A549) has both expressed CAR and MSLN. However, AdML-VTIN showed significantly higher viral copy numbers in the tumor at 48 h and 7 days (Figure 2). Although the difference was not statistically significant, we observed a certain amount of AdML-

systemically administrated AdML-VTIN accumulated and replicated in the tumor site.

We also investigated the detailed mechanism of low liver distribution of AdML-VTIN. Ad particles reach the liver through the portal vein and contact most hepatocytes only after passing through the liver sinusoids, the walls of which are formed by endothelial cells. Kupffer cells are located in the space of Disse outside of the sinusoidal wall.⁴⁶ Both hepatocytes and Kupffer cells efficiently take up Ad particles.^{25,47–49} When we separated the parenchymal cells (mainly hepatocyte) and non-parenchymal cells (including Kupffer cells), there was a significant difference between the WT virus and AdML-VTIN in the parenchymal cell fraction, but not in the non-parenchymal cell fraction. This result suggests that the decrease in the distribution of AdML-VTIN to CAR-expressing hepatocytes was the result of ablation of the CAR binding site after replacing the cancer-specific motif in the AB-loop of the fiber knob of AdML-VTIN. Several groups have reported that Ad vectors from which CAR binding has been ablated do not change the biodistribution of Ad vectors,^{50–52} because the binding of coagulation factors (e.g., FX, FIX) to the Ad5 hexon protein plays a major role in hepatocyte transduction.⁴⁵ However, several reports note that ablating the CAR binding of Ad can reduce the liver tropism. Einfeld et al. have reported that CAR binding-ablated Ad vectors exhibit a 10-fold decrease in liver transduction.⁵³ Koizumi et al. have also reported that the triple-mutant Ad vector, which ablates CAR, integrin αV , and heparan sulfate glycosaminoglycans (HSG) binding by introducing a mutation in the

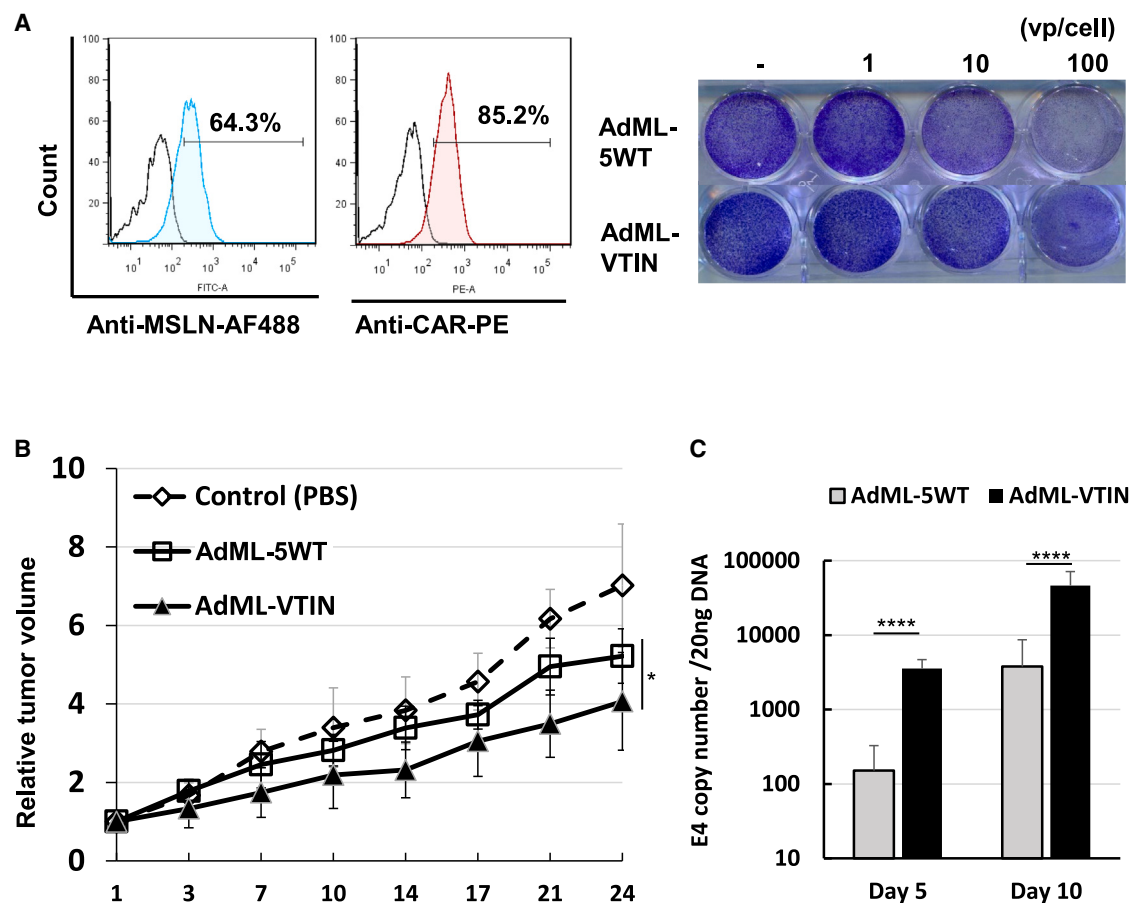


Figure 6. Anti-tumor effect of MSLN-targeted OAd with systemic injection in a pancreatic cancer model

(A) The expression level of MSLN and coxsackievirus and Ad receptor (CAR) by flow cytometry. The cytosidal effect of AdML-VTIN was assessed *in vitro* with a crystal violet assay in AsPC1 cells at 1.0, 10, and 100 vp/cell (day 6). (B) The anti-tumor effect of systemically administered MSLN-targeted OAd (3×10^9 vp/mouse) was analyzed in AsPC1 a subcutaneous xenograft model. Data are represented as mean \pm SEM; $^*p < 0.05$; one-way ANOVA followed by Tukey's multiple comparisons test; $n = 8-10$ per group. (C) At days 5 and 10, viral copy number in the tumor specimens was analyzed by qPCR. Results are shown as the E4 copy number per 20 ng DNA. The data were analyzed using a two-tailed unpaired Student's *t* test. $****p < 0.0001$; $n = 6$ for each time point.

AB-loop within the fiber knob, mediated much lower mouse liver transduction by i.v. and intraperitoneal injection than the mutant Ad vector containing a mutation in the FG-loop within the fiber knob.^{54,55} These research findings are consistent with our results of liver tropism of the MSLN-targeted OAd with AB-loop modification.

Another difficulty of systemic OAd therapy is preexisting anti-Ad nAbs. In particular, the high prevalence of a pre-existing nAb against Ad type 5 in human populations is a major limitation of systemic administration and multiple-dose regimens.⁵⁶ Although controversy remains regarding the most important Ad capsid proteins involved in the inhibition of Ad vector-mediated transduction by nAbs, previous studies reported that Ad-nAbs mainly recognize three major capsid proteins: hexon, fiber, and penton base.⁵⁷⁻⁵⁹ Tomita et al., demonstrated that anti-fiber serum significantly inhibited the *in vitro* transduction of Ad in A549 cells.⁶⁰ Anti-fiber antibodies thus appear to play an important role in nAb-mediated inhibition of

transduction with Ad vectors. Indeed, the fiber-modified OAd was more resistant to human serum, compared to fiber-unmodified OAd in an nAb assay (Figure 8A). Although further research is needed, these data suggest that OAd with a targeting motif in the AB-loop allow a degree of escape from preexisting Abs and have a greater capability to facilitate systemic therapy. Interestingly, the hemagglutination profile of the fiber-modified MSLN-targeted OAd was also changed. Although the hemagglutination-based conventional Ad group definition using rat and monkey red blood cells (RBCs) does not tell much about the hemagglutination of human RBCs, developers of therapeutics for systemic application have been trying to avoid hemagglutination because the formation of large particles eliminates the benefit of selective delivery.⁶¹ It has been reported that a major determinant of hemagglutination is the binding of knob to RBCs.⁶²⁻⁶⁵ Our data showed that the Ad5 with AB-loop modification showed far less hemagglutination compared to WT Ad5. This means tropism alternation based on

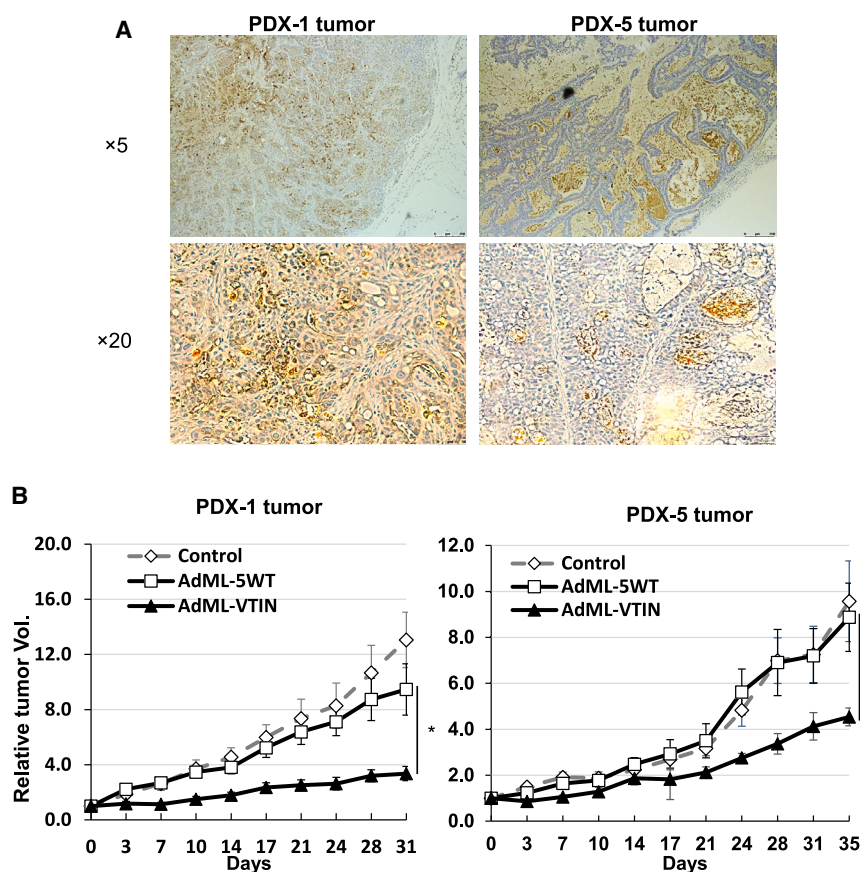


Figure 7. Anti-tumor effect of MSLN-targeted OAd in a pancreatic cancer PDX model

(A) The immunohistochemical staining of MSLN in PDX tumors (original magnification, $\times 5$ and $\times 20$). (B) The anti-tumor effect of systemically administered MSLN-targeted OAd (3×10^9 vp/mouse) was analyzed in PDX tumors originating from two different patients. Data are represented as mean \pm SEM; one-way ANOVA followed by Tukey's multiple comparisons test; PDX-1, $n = 9$ –12 per group; PDX-5, $n = 6$ –7 per group; * $p < 0.05$.

administration. Interestingly, the AB-loop modification of Ad fiber changed hemagglutination activity and became less susceptible to pre-existing nAbs in human serum. Our results indicate that an MSLN-targeted OAd is a very promising agent for the development of systemic treatment for advanced cancers.

MATERIALS AND METHODS

Cells and culture

Authenticated human lung adenocarcinoma A549 cell line was obtained from American Type Culture Collection (ATCC, Manassas, VA). We purchased new AsPC-1 cells from ATCC. After obtaining cells from ATCC, frozen cell stocks were immediately prepared and stored in a liquid nitrogen dewar. Cells were cultured for less than 6 months. Cell line

authentication was performed by ATCC using short tandem repeat DNA profiles. All cell lines were routinely maintained in ATCC-recommended conditions and cultured for experiments with Dulbecco's modified Eagle's medium with 4.5 g/L glucose, L-glutamine, and sodium pyruvate (Mediatech, Manassas, VA) and supplemented with 10% fetal bovine serum (Hyclone Thermo Scientific, Logan, UT) in a 37°C and 5% CO₂ environment under humidified conditions.

Ad design

The MSLN-targeted Ad (AdML-VTIN) has a WT E1 gene, a single *loxP* site within the E3 region, and the VTINRSA motif replacing the primary CAR-binding domain in the AB-loop of fiber knob.²⁶ The AdML-5WT, control Ad, contains a WT E1 gene, a single *loxP* site within the E3 region, and WT fiber of Ad5.²⁶ The resultant viruses with the *loxP* site are therefore E3 deficient. The titer of the viruses was determined by optical absorbance at 260 nm, qPCR, and plaque-forming assay.⁴⁰

Liver cell isolation

Liver parenchymal cells and non-parenchymal cells (including Kupffer cells) were isolated by collagenase digestion and differential centrifugation using Percoll (GE Healthcare Biosciences, Pittsburgh, PA). The detailed protocol was provided by Dr. Kenichi Ikejima and described in a paper he coauthored.³¹ Briefly, livers were perfused

AB-loop modification is an effective way to avoid hemagglutination (Figure 8B).

In this study, i.v. injection of the MSLN-targeted OAd, AdML-VTIN, showed statistically significant anti-tumor effects in MSLN⁺ pancreatic tumor models, as well as pancreatic cancer PDX models (Figures 6 and 7). The PDX model in particular represents the tumor microenvironments (TMEs) of patients and has been widely used for the evaluation of therapeutic regimens.⁶⁶ Specifically, the TME of pancreatic cancer is composed of a large stromal component consisting of cancer-associated fibroblasts, extracellular matrix, and immune cells with immunosuppressive features that act as a barrier for drug delivery.^{67,68} We think that the tumor stroma acts as a barrier that limits viral penetration and spread. However, the MSLN-targeting virus showed strong anti-tumor activity in the pancreatic cancer PDX model after systemic administration (Figure 7). These data suggest that MSLN-targeted OAds can overcome the barrier by efficient delivery to only target cancer cells without any trapping by tumor stroma cells.

In summary, systemically injected MSLN-targeted OAds showed significantly lower liver sequestration and better tumor accumulation than non-targeted OAds. Consequently, MSLN-targeted OAds showed statistically significant anti-tumor effects with systemic

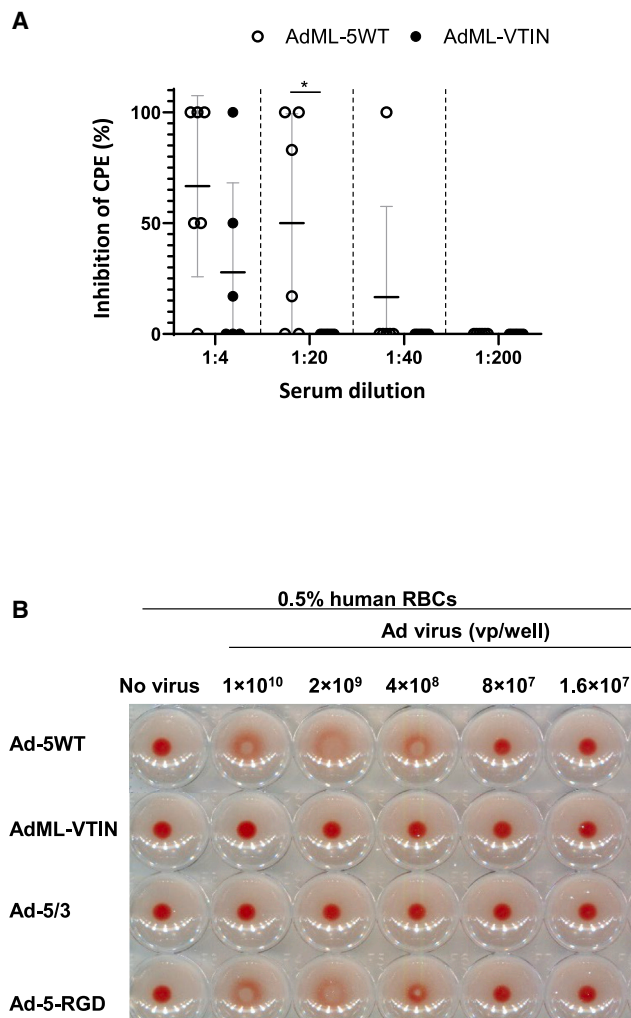


Figure 8. Neutralization and hemagglutination profile of MSLN-targeted OAd

(A) Neutralization assay by using human serum samples. The percentage of CPE⁺ wells in the presence of the diluted human serum. Data are shown as scatter dot plots, including mean and SD error bars. The data were analyzed using a two-tailed unpaired Student's *t* test; **p* < 0.05 *n* = 6 patient serum for each group. (B) Hemagglutination profiling of fiber-modified OAds. Ad5-based Ads with CAR-binding knob showed hemagglutination (Ad5 and Ad5-RGD). Replacement of the knobs with MSLN-binding motif (AdML-VTIN), or Ad3 (Ad5/3) did not cause hemagglutination.

through the portal vein with Ca²⁺- and Mg²⁺-free Hanks' balanced salt solution (HBSS) containing 0.5 mM ethylene glycol-bis (b-aminoethyl ether)-*N,N,N',N',N'',N''*-tetraacetic acid (EGTA) at 37°C for 5 min. Thereafter, perfusion was performed with HBSS containing 0.025% collagenase IV (Sigma-Aldrich, St. Louis, MO) at 37°C for 5 min. After the liver was digested, it was excised and cut into small pieces in collagenase buffer. The suspension was filtered through nylon mesh and centrifuged three times at 55 × *g* at 4°C for 3 min to collect the pellet and supernatant as the parenchymal cell fraction

and non-parenchymal cell fraction, respectively. The non-parenchymal cell fraction was washed twice with HBSS buffer.

Quantitative analysis for the adenoviral copy number

The viral solution was treated with 0.1 U/μL DNase I at 37°C for 15 min for eliminating non-capsidated viral DNA. The DNA was purified with QIAamp Blood Kit (Qiagen, Hilden, Germany) following the manufacturer's instruction. The total viral copy number was analyzed with E4 primers by SYBRGreen qPCR using the QuantiFast SYBR Green PCR Kit (Qiagen). Oligonucleotide sequences were E4-forward: 5'-GGAGTGCGCCGAGACAAC-3' and E4-reverse: 5'-ACTACGTCCGCGCTTCCAT-3'.

FACS analysis

For analysis of liver cell separation, separated cells were suspended in fluorescence-activated cell sorting (FACS) buffer, and stained with allophycocyanin-conjugated anti-F4/80 monoclonal antibody (mAb) (BioLegend, San Diego, CA) for 1 h on ice. Cells were then washed with PBS and analyzed on BD FACS Canto II flow cytometer (BD Biosciences).

For detection of MSLN expression in AsPC-1 cells, we harvested, washed, and resuspended the cells in ice-cold PBS. Primary antibody was added and incubated for 1 h on ice with anti-MSLN mAb (BioLegend, clone K1). Cells were then washed with PBS, incubated with Alexa Fluor 488 goat anti-mouse secondary antibody (Invitrogen, Carlsbad, CA) diluted to 1 μg/mL for 1 h on ice. Cells were then washed with PBS and analyzed on the BD FACS Canto II flow cytometer (BD Biosciences).

IHC for detection of MSLN expression in tumor

Formalin-fixed paraffin-embedded A549, AsPC1, and PDX tumors were stained with an anti-MSLN mAb (5B2, dilution 1/20; Thermo Fisher Scientific, Waltham, MA) overnight at 4°C. Signals were visualized with IHC Select HRP/DAB kit (Millipore, Burlington, MA).

In vivo vector distribution

To analyze vector distribution *in vivo*, 5 × 10⁶ of A549 cells were inoculated subcutaneously into the flanks of female nude mice, and 1 × 10¹⁰ vp of the selected virus or control virus was systemically injected when the diameter reached 5–7 mm. Mice were sacrificed 1 h, 48 h, and 7 days after injection. DNA was purified from frozen tumor tissue using the DNeasy Blood & Tissue Kit (Qiagen), and the adenoviral DNA copy number of the E4 region was quantified by qPCR starting from 20 ng DNA. The animal experiments were performed in accordance with the institutionally approved animal experimental protocol.

In vivo therapeutic effect in established tumors

To analyze the anti-tumor effect in an *in vivo* model, 5 × 10⁶ of A549 or AsPC1 cells were inoculated subcutaneously into the flanks of the female nude mice, and 3 × 10⁹ vp/mouse of AdML-VTIN virus or control AdML-5WT virus was injected systemically or i.t. when the diameter reached 5–7 mm. To establish pancreatic cancer PDX

models, de-identified fresh human primary pancreatic cancer samples that were pathologically diagnosed with adenocarcinoma were obtained within 30 min of surgical resection from the Tissue Procurement Facility (University of Minnesota). After dissection and removal of the necrotic areas, fatty tissues, blood clots and connective tissues with forceps and scissors, each tumor specimen was cut into $2 \times 2 \times 2$ -mm pieces. Immediately following this process, a small piece of the tumor was implanted subcutaneously in the flanks of 8-week-old NOD/SCID mice (The Jackson Laboratory, Bar Harbor, ME) and maintained by re-transplantation. When the tumor size reached 5–7 mm in diameter, 3×10^9 vp/mouse of AdML-VTIN virus or control AdML-5WT virus was systemically injected. The condition of the mice was monitored daily, and the tumor diameter was measured twice per week. The tumor volume was calculated as $\text{width}^2 \times \text{length} / 2$.

In a separate experiment under the same conditions, the mice were sacrificed at various time points. The DNA was purified from frozen tumor tissues by using the QIAamp DNA Mini Kit, and the adenoviral DNA copy number of the E4 region was quantified by qPCR starting from 20 ng DNA. The expression of adenoviral hexon protein in the tumor was analyzed by immunostaining.^{26,69} All slides were scanned with a $10\times$ objective lens magnification using a Nikon Eclipse TS100 microscope.

Multiple injection assay

At day 47, when the average of the tumor volume reached 500 mm^3 , multiple time point injections of AdML-VTIN against regrown tumors started. AdML-VTIN via i.v. injection (3×10^9 vp/mouse) was performed at days 47, 61, 68, 75, and 82. The condition of the mice was monitored daily, and the tumor diameter was measured twice per week.

Neutralization assay

For the neutralization assay with the MSLN-targeted OAd, A549 (human lung carcinoma) cells were seeded in to 96-well plates at 5×10^4 cells in 100 μL culture media. On the following day, human serum was heat inactivated at 56°C for 60 min before a serial dilution was performed in a 96-well tissue culture plate. The serum was serially diluted and mixed with 100 TCID₅₀ of Ads (Ad5-WT or AdML-VTIN). After a 30-min incubation at 37°C , A549 cells were infected with the virus/serum mixture. After 7 days of incubation, the number of wells that are positive for cytopathic effect (CPE) was scored and the CPE positivity was calculated.

Hemagglutination assay

Erythrocytes were extracted from blood cells derived from a human donor, who gave informed consent. Then, 50 μL of 0.5% (v/v) erythrocyte suspension was layered in each well of the concave-bottom-shaped 96-well plate, and 50 μL virus dilutions (1×10^{10} vp– 2.56×10^4 vp in PBS) was added and gently mixed into the erythrocyte suspension. The plates were incubated at 37°C for 2 h to allow sedimentation to occur. Hemagglutination was assessed visually.

Statistical analysis

Statistical analysis was performed using GraphPad Prism (version 10, GraphPad, La Jolla, CA). Comparisons between two groups were performed using two-tailed unpaired Student's *t* tests. Comparison between more than two groups was performed by ANOVA with a multiple comparison test. Results are expressed as mean \pm SD or SEM, and differences with $p < 0.05$ were considered statistically significant.

DATA AVAILABILITY

The data that support the findings of our study are available from the corresponding author upon reasonable request.

ACKNOWLEDGMENTS

This work was supported by the National Institutes of Health (R01CA276480, R01CA228760, R01CA168448, and R01CA196215 to M.Y.), and the National Science Foundation (NSF I-Corps award 2120068 to P.H.). We thank B.R. for comments and assistance with the manuscript. The graphical abstract was partially created in BioRender (<https://BioRender.com/d60u474>).

AUTHOR CONTRIBUTIONS

Design of research studies, M.S.-D., Y.M., and M.Y.; conduct of experiments, M.S.-D. and M.Y.; acquisition of data, M.S.-D., Y.M., K.J., and B.R.; analysis of data, M.S.-D., and Y.M.; provision of reagents, M.S.-D. and P.H.; manuscript preparation, M.S.-D.; manuscript review and editing, all authors.

DECLARATION OF INTERESTS

Y.M., and M.Y. are described as inventors in a patent application for the Ad library system ("Adenovirus Library and Methods"), which was filed in the US Patent and Trademark Office as US-10208304-B2. M.S.-D., P.H., and M.Y. are described as inventors in a patent application ("Adenovirus Constructs and Methods of Use"), which was filed in the US Patent and Trademark Office as PCT/US2023/017811.

SUPPLEMENTAL INFORMATION

Supplemental information can be found online at <https://doi.org/10.1016/j.omton.2025.200967>.

REFERENCES

- Wagner, P.D., Maruvada, P., and Srivastava, S. (2004). Molecular diagnostics: a new frontier in cancer prevention. *Mol. Diagn.* 4, 503–511.
- Bathen, T.F., Sitter, B., Sjøbakk, T.E., Tessem, M.B., and Gribbestad, I.S. (2010). Magnetic resonance metabolomics of intact tissue: A biotechnological tool in cancer diagnostics and treatment evaluation. *Cancer Res.* 70, 6692–6696. <https://doi.org/10.1158/0008-5472.CAN-10-0437>.
- Chen, V.W., Ruiz, B.A., Hsieh, M.C., Wu, X.C., Ries, L.A.G., and Lewis, D.R. (2014). Analysis of stage and clinical/prognostic factors for lung cancer from SEER registries: AJCC staging and collaborative stage data collection system. *Cancer* 120, 3781–3792. <https://doi.org/10.1002/cncr.29045>.
- SEER*Explorer (2021). An interactive website for SEER cancer statistics [Internet]. <https://seer.cancer.gov/statistics-network/explorer/>.
- Rahib, L., Smith, B.D., Aizenberg, R., Rosenzweig, A.B., Fleshman, J.M., and Matrisian, L.M. (2014). Projecting Cancer Incidence and Deaths to 2030: The Unexpected Burden of Thyroid, Liver, and Pancreas Cancers in the United States. *Cancer Res.* 74, 2913–2921. <https://doi.org/10.1158/0008-5472.CAN-14-0155>.
- American Cancer, S. (2019). Facts & Figures 2019 (American Cancer Society).
- Andtbacka, R.H.I., Kaufman, H.L., Collichio, F., Amatruda, T., Senzer, N., Chesney, J., Delman, K.A., Spitler, L.E., Puzanov, I., Agarwala, S.S., et al. (2015). Talimogene Laherparepvec Improves Durable Response Rate in Patients With Advanced Melanoma. *J. Clin. Oncol.* 33, 2780–2788. <https://doi.org/10.1200/JCO.2014.58.3377>.

8. Yamamoto, M., and Yamamoto, M. (2004). Conditionally replicative adenovirus for gastrointestinal cancers. *Exp. Opin. Biol. Ther.* 4, 1241–1250. <https://doi.org/10.1517/14712598.4.8.1241>.
9. Yamamoto, M., and Curiel, D.T. (2010). Current Issues and Future Directions of Oncolytic Adenoviruses. *Mol. Ther.* 18, 243–250. <https://doi.org/10.1038/mt.2009.266>.
10. Bischoff, J.R., Kirn, D.H., Williams, A., Heise, C., Horn, S., Muna, M., Ng, L., Nye, J.A., Sampson-Johannes, A., Fattaey, A., and McCormick, F. (1996). An Adenovirus Mutant That Replicates Selectively in p53- Deficient Human Tumor Cells. *Science* 274, 373–376. <https://doi.org/10.1126/science.274.5286.373>.
11. Southam, C.M., and Moore, A.E. (1952). Clinical studies of viruses as antineoplastic agents, with particular reference to Egypt 101 virus. *Cancer* 5, 1025–1034.
12. Southam, C.M., and Moore, A.E. (1954). Induced virus infection in man by Egypt isolated of west Nile virus. *Am. J. Trop. Med. Hyg.* 3, 19–50.
13. Telerman, A., Tuynder, M., Dupressoir, T., Robaye, B., Sigaux, F., Shaulian, E., Oren, M., Rommelaere, J., and Amson, R. (1993). A model for tumor suppression using H-1 parvovirus. *Proc. Natl. Acad. Sci. USA* 90, 8702–8706. <https://doi.org/10.1073/pnas.90.18.8702>.
14. Martuza, R.L., Malick, A., Markert, J.M., Ruffner, K.L., and Coen, D.M. (1991). Experimental therapy of human glioma by means of a genetically engineered virus mutant. *Science* 252, 854–856.
15. Markert, J.M., Malick, A., Coen, D.M., and Martuza, R.L. (1993). Reduction and elimination of encephalitis in an experimental glioma therapy model with attenuated herpes simplex mutants that retain susceptibility to acyclovir. *Neurosurgery* 32, 597–603. <https://doi.org/10.1227/00006123-199304000-00016>.
16. Mineta, T., Rabkin, S.D., and Martuza, R.L. (1994). Treatment of malignant gliomas using ganciclovir-hypersensitive, ribonucleotide reductase-deficient herpes simplex viral mutant. *Cancer Res.* 54, 3963–3966.
17. Chambers, R., Gillespie, G.Y., Sorocanu, L., Andreansky, S., Chatterjee, S., Chou, J., Roizman, B., and Whitley, R.J. (1995). Comparison of genetically engineered herpes simplex viruses for the treatment of brain tumors in a scid mouse model of human malignant glioma. *Proc. Natl. Acad. Sci. USA* 92, 1411–1415.
18. Markert, J.M., Coen, D.M., Malick, A., Mineta, T., and Martuza, R.L. (1992). Expanded spectrum of viral therapy in the treatment of nervous system tumors. *J. Neurosurg.* 77, 590–594.
19. Russell, S.J. (2002). RNA viruses as virotherapy agents. *Cancer Gene Ther.* 9, 961–966.
20. Shenk, T. (1996). In *Adenoviridae: The Viruses and Their Replication*, K.D. Virology, B. Fields, and P. Howley, eds. (Philadelphia, PA, USA: Lipponcott-Raven), pp. 2111–2148.
21. Sato-Dahlman, M., and Yamamoto, M. (2018). The Development of Oncolytic Adenovirus Therapy in the Past and Future - For the Case of Pancreatic Cancer. *Curr. Cancer Drug Targets* 18, 153–161. <https://doi.org/10.2174/1568009617666170222123925>.
22. Nattress, C.B., and Halldén, G. (2018). Advances in oncolytic adenovirus therapy for pancreatic cancer. *Cancer Lett.* 434, 56–69.
23. Sato-Dahlman, M., Wirth, K., and Yamamoto, M. (2018). Role of gene therapy in pancreatic cancer—A review. *Cancers* 10, 103.
24. Lozier, J.N., Csako, G., Mondoro, T.H., Krizek, D.M., Metzger, M.E., Costello, R., Vostal, J.G., Rick, M.E., Donahue, R.E., and Morgan, R.A. (2002). Toxicity of a first-generation adenoviral vector in rhesus macaques. *Hum. Gene Ther.* 13, 113–124. <https://doi.org/10.1089/10430340152712665>.
25. Alemany, R., Suzuki, K., and Curiel, D.T. (2000). Blood clearance rates of adenovirus type 5 in mice. *J. Gen. Virol.* 81, 2605–2609. <https://doi.org/10.1099/0022-1317-81-11-2605>.
26. Miura, Y., Yamasaki, S., Davydova, J., Brown, E., Aoki, K., Vickers, S., and Yamamoto, M. (2013). Infectivity-selective oncolytic adenovirus developed by high-throughput screening of adenovirus-formatted library. *Mol. Ther.* 21, 139–148. <https://doi.org/10.1038/mt.2012.205>.
27. Frierson, H.F., Jr., Moskaluk, C.A., Powell, S.M., Zhang, H., Cerilli, L.A., Stoler, M.H., Cathro, H., and Hampton, G.M. (2003). Large-scale molecular and tissue microarray analysis of mesothelin expression in common human carcinomas. *Hum. Pathol.* 34, 605–609. [https://doi.org/10.1016/s0046-8177\(03\)00177-1](https://doi.org/10.1016/s0046-8177(03)00177-1).
28. Hassan, R., Bera, T., and Pastan, I. (2004). Mesothelin: a new target for immunotherapy. *Clin. Cancer Res.* 10, 3937–3942. <https://doi.org/10.1158/1078-0432.CCR-03-0801>.
29. Chang, K., and Pastan, I. (1996). Molecular cloning of mesothelin, a differentiation antigen present on mesothelium, mesotheliomas, and ovarian cancers. *Proc. Natl. Acad. Sci. USA* 93, 136–140. <https://doi.org/10.1073/pnas.93.1.136>.
30. Ho, M., Bera, T.K., Willingham, M.C., Onda, M., Hassan, R., FitzGerald, D., and Pastan, I. (2007). Mesothelin expression in human lung cancer. *Clin. Cancer Res.* 13, 1571–1575. <https://doi.org/10.1158/1078-0432.CCR-06-2161>.
31. Fukada, H., Yamashina, S., Izumi, K., Komatsu, M., Tanaka, K., Ikejima, K., and Watanabe, S. (2012). Suppression of autophagy sensitizes Kupffer cells to endotoxin. *Hepatology* 55, 1112–1118. <https://doi.org/10.1111/j.1872-034X.2012.01024.x>.
32. Sirena, D., Lilienfeld, B., Eisenhut, M., Kälin, S., Boucke, K., Beerli, R.R., Vogt, L., Ruedl, C., Bachmann, M.F., Greber, U.F., and Hemmi, S. (2004). The human membrane cofactor CD46 is a receptor for species B adenovirus serotype 3. *J. Virol.* 78, 4454–4462. <https://doi.org/10.1128/JVI.78.9.4454-4462.2004>.
33. Wang, H., Li, Z.-Y., Liu, Y., Persson, J., Beyer, I., Möller, T., Koyuncu, D., Drescher, M.R., Strauss, R., Zhang, X.-B., et al. (2011). Desmoglein 2 is a receptor for adenovirus serotypes 3, 7, 11 and 14. *Nat. Med.* 17, 96–104. <https://doi.org/10.1038/nm.2270>.
34. Kass-Eisler, A., Falck-Pedersen, E., Elfenbein, D.H., Alvira, M., Buttrick, P.M., and Leinwand, L.A. (1994). The impact of developmental stage, route of administration and the immune system on adenovirus-mediated gene transfer. *Gene Ther.* 1, 395–402.
35. Bernt, K.M., Ni, S., Gaggari, A., Li, Z.Y., Shayakhmetov, D.M., and Lieber, A. (2003). The effect of sequestration by nontarget tissues on anti-tumor efficacy of systemically applied, conditionally replicating adenovirus vectors. *Mol. Ther.* 8, 746–755. <https://doi.org/10.1016/j.ymthe.2003.07.006>.
36. Vrancken Peeters, M.J., Perkins, A.L., and Kay, M.A. (1996). Method for multiple portal vein infusions in mice: quantitation of adenovirus-mediated hepatic gene transfer. *Biotechniques* 20, 278–285. <https://doi.org/10.2144/96202rr05>.
37. Thomas, C.E., Ehrhardt, A., and Kay, M.A. (2003). Progress and problems with the use of viral vectors for gene therapy. *Nat. Rev. Genet.* 4, 346–358. <https://doi.org/10.1038/nrg1066>.
38. Pearson, A.S., Koch, P.E., Atkinson, N., Xiong, M., Finberg, R.W., Roth, J.A., and Fang, B. (1999). Factors limiting adenovirus-mediated gene transfer into human lung and pancreatic cancer cell lines. *Clin. Cancer Res.* 5, 4208–4213.
39. Davydova, J., Le, L.P., Gavrikova, T., Wang, M., Krasnykh, V., and Yamamoto, M. (2004). Infectivity-enhanced cyclooxygenase-2-based conditionally replicative adenoviruses for esophageal adenocarcinoma treatment. *Cancer Res.* 64, 4319–4327. <https://doi.org/10.1158/0008-5472.CAN-04-0064>.
40. Yamamoto, M., Davydova, J., Wang, M., Siegal, G.P., Krasnykh, V., Vickers, S.M., and Curiel, D.T. (2003). Infectivity enhanced, cyclooxygenase-2 promoter-based conditionally replicative adenovirus for pancreatic cancer. *Gastroenterology* 125, 1203–1218. [https://doi.org/10.1016/s0016-5085\(03\)01196-x](https://doi.org/10.1016/s0016-5085(03)01196-x).
41. Krasnykh, V.N., Mikheeva, G.V., Douglas, J.T., and Curiel, D.T. (1996). Generation of recombinant adenovirus vectors with modified fibers for altering viral tropism. *J. Virol.* 70, 6839–6846.
42. Chen, L., Liu, Q., Qin, R., Le, H., Xia, R., Li, W., and Kumar, M. (2005). Amplification and functional characterization of MUC1 promoter and gene-virotherapy via a targeting adenoviral vector expressing hSTR2 gene in MUC1-positive Panc-1 pancreatic cancer cells in vitro. *Int. J. Mol. Med.* 15, 617–626.
43. Heise, C., Sampson-Johannes, A., Williams, A., McCormick, F., Von Hoff, D.D., and Kirn, D.H. (1997). ONYX-015, an E1B gene-attenuated adenovirus, causes tumor-specific cytolysis and antitumoral efficacy that can be augmented by standard chemotherapeutic agents. *Nat. Med.* 3, 639–645. <https://doi.org/10.1038/nm0697-639>.
44. Fueyo, J., Gomez-Manzano, C., Alemany, R., Lee, P.S., McDonnell, T.J., Mitlianga, P., Shi, Y.X., Levin, V.A., Yung, W.K., and Kyritsis, A.P. (2000). A mutant oncolytic adenovirus targeting the Rb pathway produces anti-glioma effect in vivo. *Oncogene* 19, 2–12. <https://doi.org/10.1038/sj.onc.1203251>.

45. Shayakhmetov, D.M., Gaggar, A., Ni, S., Li, Z.-Y., and Lieber, A. (2005). Adenovirus binding to blood factors results in liver cell infection and hepatotoxicity. *J. Virol.* 79, 7478–7491. <https://doi.org/10.1128/JVI.79.12.7478-7491.2005>.
46. Bonnardel, J., T'Jonck, W., Gaublomme, D., Browaeys, R., Scott, C.L., Martens, L., Vanneste, B., De Prijck, S., Nedospasov, S.A., Kremer, A., et al. (2019). Stellate Cells, Hepatocytes, and Endothelial Cells Imprint the Kupffer Cell Identity on Monocytes Colonizing the Liver Macrophage Niche. *Immunity* 51, 638–654.e639. <https://doi.org/10.1016/j.immuni.2019.08.017>.
47. Shayakhmetov, D.M., Li, Z.-Y., Ni, S., and Lieber, A. (2004). Analysis of adenovirus sequestration in the liver, transduction of hepatic cells, and innate toxicity after injection of fiber-modified vectors. *J. Virol.* 78, 5368–5381. <https://doi.org/10.1128/jvi.78.10.5368-5381.2004>.
48. Lieber, A., He, C.Y., Meuse, L., Schowalter, D., Kirillova, I., Winther, B., and Kay, M.A. (1997). The role of Kupffer cell activation and viral gene expression in early liver toxicity after infusion of recombinant adenovirus vectors. *J. Virol.* 71, 8798–8807. <https://doi.org/10.1128/JVI.71.11.8798-8807.1997>.
49. Schiedner, G., Hertel, S., Johnston, M., Dries, V., van Rooijen, N., and Kochanek, S. (2003). Selective depletion or blockade of Kupffer cells leads to enhanced and prolonged hepatic transgene expression using high-capacity adenoviral vectors. *Mol. Ther.* 7, 35–43. [https://doi.org/10.1016/s1525-0016\(02\)00017-5](https://doi.org/10.1016/s1525-0016(02)00017-5).
50. Alemany, R., and Curiel, D.T. (2001). CAR-binding ablation does not change bio-distribution and toxicity of adenoviral vectors. *Gene Ther.* 8, 1347–1353. <https://doi.org/10.1038/sj.gt.3301515>.
51. Leissner, P., Legrand, V., Schlesinger, Y., Hadji, D.A., van Raaij, M., Cusack, S., Pavirani, A., and Mehtali, M. (2001). Influence of adenoviral fiber mutations on viral encapsidation, infectivity and in vivo tropism. *Gene Ther.* 8, 49–57. <https://doi.org/10.1038/sj.gt.3301343>.
52. Mizuguchi, H., Koizumi, N., Hosono, T., Ishii-Watabe, A., Uchida, E., Utoguchi, N., Watanabe, Y., and Hayakawa, T. (2002). CAR- or alphav integrin-binding ablated adenovirus vectors, but not fiber-modified vectors containing RGD peptide, do not change the systemic gene transfer properties in mice. *Gene Ther.* 9, 769–776. <https://doi.org/10.1038/sj.gt.3301701>.
53. Einfeld, D.A., Schroeder, R., Roelvink, P.W., Lizonova, A., King, C.R., Kovesdi, I., and Wickham, T.J. (2001). Reducing the native tropism of adenovirus vectors requires removal of both CAR and integrin interactions. *J. Virol.* 75, 11284–11291. <https://doi.org/10.1128/JVI.75.23.11284-11291.2001>.
54. Koizumi, N., Mizuguchi, H., Sakurai, F., Yamaguchi, T., Watanabe, Y., and Hayakawa, T. (2003). Reduction of natural adenovirus tropism to mouse liver by fiber-shaft exchange in combination with both CAR- and alphav integrin-binding ablation. *J. Virol.* 77, 13062–13072. <https://doi.org/10.1128/jvi.77.24.13062-13072.2003>.
55. Koizumi, N., Kawabata, K., Sakurai, F., Watanabe, Y., Hayakawa, T., and Mizuguchi, H. (2006). Modified adenoviral vectors ablated for coxsackievirus-adenovirus receptor, alphav integrin, and heparan sulfate binding reduce in vivo tissue transduction and toxicity. *Hum. Gene Ther.* 17, 264–279. <https://doi.org/10.1089/hum.2006.17.264>.
56. Nwanegbo, E., Vardas, E., Gao, W., Whittle, H., Sun, H., Rowe, D., Robbins, P.D., and Gambotto, A. (2004). Prevalence of neutralizing antibodies to adenoviral serotypes 5 and 35 in the adult populations of The Gambia, South Africa, and the United States. *Clin. Diagn. Lab. Immunol.* 11, 351–357. <https://doi.org/10.1128/cdli.11.2.351-357.2004>.
57. Yu, B., Dong, J., Wang, C., Zhan, Y., Zhang, H., Wu, J., Kong, W., and Yu, X. (2013). Characteristics of neutralizing antibodies to adenovirus capsid proteins in human and animal sera. *Virology* 437, 118–123. <https://doi.org/10.1016/j.virol.2012.12.014>.
58. Sumida, S.M., Truitt, D.M., Lemckert, A.A.C., Vogels, R., Custers, J.H.H.V., Addo, M.M., Lockman, S., Peter, T., Peyerl, F.W., Kishko, M.G., et al. (2005). Neutralizing Antibodies to Adenovirus Serotype 5 Vaccine Vectors Are Directed Primarily against the Adenovirus Hexon Protein. *J. Immunol.* 174, 7179–7185. <https://doi.org/10.4049/jimmunol.174.11.7179>.
59. Hong, S.S., Habib, N.A., Franqueville, L., Jensen, S., and Boulanger, P.A. (2003). Identification of Adenovirus (Ad) Penton Base Neutralizing Epitopes by Use of Sera from Patients Who Had Received Conditionally Replicative Ad (Add1520) for Treatment of Liver Tumors. *J. Virol.* 77, 10366–10375. <https://doi.org/10.1128/JVI.77.19.10366-10375.2003>.
60. Tomita, K., Sakurai, F., Iizuka, S., Hemmi, M., Wakabayashi, K., Machitani, M., Tachibana, M., Katayama, K., Kamada, H., and Mizuguchi, H. (2018). Antibodies against adenovirus fiber and penton base proteins inhibit adenovirus vector-mediated transduction in the liver following systemic administration. *Sci. Rep.* 8, 12315. <https://doi.org/10.1038/s41598-018-30947-z>.
61. Li, C., and Lieber, A. (2019). Adenovirus vectors in hematopoietic stem cell genome editing. *FEBS Lett.* 593, 3623–3648. <https://doi.org/10.1002/1873-3468.13668>.
62. Carlisle, R.C., Di, Y., Cerny, A.M., Sonnen, A.F.P., Sim, R.B., Green, N.K., Subr, V., Ulbrich, K., Gilbert, R.J.C., Fisher, K.D., et al. (2009). Human erythrocytes bind and inactivate type 5 adenovirus by presenting Coxsackie virus-adenovirus receptor and complement receptor 1. *Blood* 113, 1909–1918. <https://doi.org/10.1182/blood-2008-09-178459>.
63. Nicol, C.G., Graham, D., Miller, W.H., White, S.J., Smith, T.A.G., Nicklin, S.A., Stevenson, S.C., and Baker, A.H. (2004). Effect of adenovirus serotype 5 fiber and penton modifications on in vivo tropism in rats. *Mol. Ther.* 10, 344–354. <https://doi.org/10.1016/j.ymthe.2004.05.020>.
64. Madisch, I., Harste, G., Pommer, H., and Heim, A. (2005). Phylogenetic analysis of the main neutralization and hemagglutination determinants of all human adenovirus prototypes as a basis for molecular classification and taxonomy. *J. Virol.* 79, 15265–15276. <https://doi.org/10.1128/JVI.79.24.15265-15276.2005>.
65. Seiradake, E., Henaff, D., Wodrich, H., Billet, O., Perreau, M., Hippert, C., Mennechet, F., Schoehn, G., Lortat-Jacob, H., Dreja, H., et al. (2009). The cell adhesion molecule "CAR" and sialic acid on human erythrocytes influence adenovirus in vivo biodistribution. *PLoS Pathog.* 5, e1000277. <https://doi.org/10.1371/journal.ppat.1000277>.
66. Tentler, J.J., Tan, A.C., Weekes, C.D., Jimeno, A., Leong, S., Pitts, T.M., Arcaroli, J.J., Messersmith, W.A., and Eckhardt, S.G. (2012). Patient-derived tumour xenografts as models for oncology drug development. *Nat. Rev. Clin. Oncol.* 9, 338–350. <https://doi.org/10.1038/nrclinonc.2012.61>.
67. Ryan, D.P., Hong, T.S., and Bardeesy, N. (2014). Pancreatic adenocarcinoma. *N. Engl. J. Med.* 371, 1039–1049. <https://doi.org/10.1056/NEJMra1404198>.
68. Feig, C., Gopinathan, A., Neesse, A., Chan, D.S., Cook, N., and Tuveson, D.A. (2012). The pancreas cancer microenvironment. *Clin. Cancer Res.* 18, 4266–4276. <https://doi.org/10.1158/1078-0432.CCR-11-3114>.
69. Sato-Dahlman, M., Miura, Y., Huang, J.L., Hajeri, P., Jacobsen, K., Davydova, J., and Yamamoto, M. (2017). CD133-targeted oncolytic adenovirus demonstrates anti-tumor effect in colorectal cancer. *Oncotarget* 8, 76044–76056. <https://doi.org/10.18632/oncotarget.18340>.